

Search for baryon-number and lepton-number violating decays $D^0 \rightarrow \bar{p}e^+$ and $D^0 \rightarrow pe^-$

M. Ablikim¹, M. N. Achasov^{10,b}, P. Adlarson⁶⁷, S. Ahmed¹⁵, M. Albrecht⁴, R. Aliberti²⁸, A. Amoroso^{66A,66C}, M. R. An³², Q. An^{63,49}, X. H. Bai⁵⁷, Y. Bai⁴⁸, O. Bakina²⁹, R. Baldini Ferroli^{23A}, I. Balossino^{24A}, Y. Ban^{38,g}, K. Begzsuren²⁶, N. Berger²⁸, M. Bertani^{23A}, D. Bettoni^{24A}, F. Bianchi^{66A,66C}, J. Bloms⁶⁰, A. Bortone^{66A,66C}, I. Boyko²⁹, R. A. Briere⁵, A. Brueggemann⁶⁰, H. Cai⁶⁸, X. Cai^{1,49}, A. Calcaterra^{23A}, G. F. Cao^{1,54}, N. Cao^{1,54}, S. A. Cetin^{53A}, J. F. Chang^{1,49}, W. L. Chang^{1,54}, G. Chelkov^{29,a}, G. Chen¹, H. S. Chen^{1,54}, M. L. Chen^{1,49}, S. J. Chen³⁵, X. R. Chen^{25,54}, Y. B. Chen^{1,49}, Z. J. Chen^{20,h}, W. S. Cheng^{66C}, G. Cibinetto^{24A}, F. Cossio^{66C}, H. L. Dai^{1,49}, J. P. Dai^{42,e}, X. C. Dai^{1,54}, A. Dbeyssi¹⁵, R. E. de Boer⁴, D. Dedovich²⁹, Z. Y. Deng¹, A. Denig²⁸, I. Denysenko²⁹, M. Destefanis^{66A,66C}, F. De Mori^{66A,66C}, Y. Ding³³, J. Dong^{1,49}, L. Y. Dong^{1,54}, M. Y. Dong^{1,49,54}, X. Dong⁶⁸, S. X. Du⁷¹, Y. L. Fan⁶⁸, J. Fang^{1,49}, S. S. Fang^{1,54}, Y. Fang¹, R. Farinelli^{24A}, L. Fava^{66B,66C}, F. Feldbauer⁴, G. Felici^{23A}, C. Q. Feng^{63,49}, J. H. Feng⁵⁰, M. Fritsch⁴, C. D. Fu¹, Y. N. Gao^{38,g}, Ya Gao⁶⁴, Yang Gao^{63,49}, I. Garzia^{24A,24B}, P. T. Ge⁶⁸, C. Geng⁵⁰, E. M. Gersabeck⁵⁸, A. Gilman⁶¹, K. Goetzen¹¹, L. Gong³³, W. X. Gong^{1,49}, W. Gradl²⁸, M. Greco^{66A,66C}, L. M. Gu³⁵, M. H. Gu^{1,49}, Y. T. Gu¹³, C. Y. Guan^{1,54}, L. B. Guo³⁴, R. P. Guo⁴⁰, Y. P. Guo^{9,f}, A. Guskov^{29,a}, T. T. Han⁴¹, W. Y. Han³², X. Q. Hao¹⁶, F. A. Harris⁵⁶, K. L. He^{1,54}, F. H. Heinsius⁴, C. H. Heinz²⁸, Y. K. Heng^{1,49,54}, C. Herold⁵¹, M. Himmelreich^{11,d}, T. Holtmann⁴, G. Y. Hou^{1,54}, Y. R. Hou⁵⁴, Z. L. Hou¹, H. M. Hu^{1,54}, J. F. Hu^{47,i}, T. Hu^{1,49,54}, Y. Hu¹, G. S. Huang^{63,49}, L. Q. Huang⁶⁴, X. T. Huang⁴¹, Y. P. Huang¹, Z. Huang^{38,g}, T. Hussain⁶⁵, N. Hüskén^{22,28}, W. Imoehl²², M. Irshad^{63,49}, J. Jackson²², S. Jaeger⁴, S. Janchiv²⁶, Q. Ji¹, Q. P. Ji¹⁶, X. B. Ji^{1,54}, X. L. Ji^{1,49}, Y. Y. Ji⁴¹, H. B. Jiang⁴¹, X. S. Jiang^{1,49,54}, Y. Jiang⁵⁴, J. B. Jiao⁴¹, Z. Jiao¹⁸, S. Jin³⁵, Y. Jin⁵⁷, M. Q. Jing^{1,54}, T. Johansson⁶⁷, N. Kalantar-Nayestanaki⁵⁵, X. S. Kang³³, R. Kappert⁵⁵, M. Kavatsyuk⁵⁵, B. C. Ke⁷¹, I. K. Keshk⁴, A. Khoukaz⁶⁰, P. Kiese²⁸, R. Kiuchi¹, R. Kliemt¹¹, L. Koch³⁰, O. B. Kolcu^{53A}, B. Kopf⁴, M. Kuemmel⁴, M. Kuessner⁴, A. Kupsc⁶⁷, M. G. Kurth^{1,54}, W. Kühn³⁰, J. J. Lane⁵⁸, J. S. Lange³⁰, P. Larin¹⁵, A. Lavania²¹, L. Lavezzi^{66A,66C}, Z. H. Lei^{63,49}, H. Leithoff²⁸, M. Lellmann²⁸, T. Lenz²⁸, C. Li³⁹, C. H. Li³², Cheng Li^{63,49}, D. M. Li⁷¹, F. Li^{1,49}, G. Li¹, H. Li^{63,49}, H. Li⁴³, H. B. Li^{1,54}, H. J. Li¹⁶, J. Q. Li⁴, J. S. Li⁵⁰, J. W. Li⁴¹, Ke Li¹, L. K. Li¹, Lei Li³, P. R. Li^{31,j,k}, S. Y. Li⁵², W. D. Li^{1,54}, W. G. Li¹, X. H. Li^{63,49}, X. L. Li⁴¹, Xiaoyu Li^{1,54}, Z. Y. Li⁵⁰, H. Liang^{63,49}, H. Liang²⁷, H. Liang^{1,54}, Y. F. Liang⁴⁵, Y. T. Liang^{25,54}, G. R. Liao¹², L. Z. Liao^{1,54}, L. Z. Liao⁴¹, J. Libby²¹, A. Limphirat⁵¹, C. X. Lin⁵⁰, B. J. Liu¹, C. X. Liu¹, D. Liu^{15,63}, F. H. Liu⁴⁴, Fang Liu¹, Feng Liu⁶, H. B. Liu¹³, H. M. Liu^{1,54}, Huanhuan Liu¹, Huihui Liu¹⁷, J. B. Liu^{63,49}, J. L. Liu⁶⁴, J. Y. Liu^{1,54}, K. Liu¹, K. Y. Liu³³, L. Liu^{63,49}, M. H. Liu^{9,f}, P. L. Liu¹, Q. Liu⁶⁸, Q. Liu⁵⁴, S. B. Liu^{63,49}, Shuai Liu⁴⁶, T. Liu^{1,54}, W. M. Liu^{63,49}, X. Liu^{31,j,k}, Y. Liu^{31,j,k}, Y. B. Liu³⁶, Z. A. Liu^{1,49,54}, Z. Q. Liu⁴¹, X. C. Lou^{1,49,54}, F. X. Lu⁵⁰, H. J. Lu¹⁸, J. D. Lu^{1,54}, J. G. Lu^{1,49}, X. L. Lu¹, Y. Lu¹, Y. P. Lu^{1,49}, C. L. Luo³⁴, M. X. Luo⁷⁰, T. Luo^{9,f}, X. L. Luo^{1,49}, X. R. Lyu⁵⁴, F. C. Ma³³, H. L. Ma¹, L. L. Ma⁴¹, M. M. Ma^{1,54}, Q. M. Ma¹, R. Q. Ma^{1,54}, R. T. Ma⁵⁴, X. X. Ma^{1,54}, X. Y. Ma^{1,49}, Y. Ma^{38,g}, F. E. Maas¹⁵, M. Maggiora^{66A,66C}, S. Maldaner⁴, S. Malde⁶¹, Q. A. Malik⁶⁵, A. Mangoni^{23B}, Y. J. Mao^{38,g}, Z. P. Mao¹, S. Marcello^{66A,66C}, Z. X. Meng⁵⁷, J. G. Messchendorp^{55,11}, G. Mezzadri^{24A}, T. J. Min³⁵, R. E. Mitchell²², X. H. Mo^{1,49,54}, N. Yu. Muchnoi^{10,b}, H. Muramatsu⁵⁹, S. Nakhoul^{11,d}, Y. Nefedov²⁹, F. Nerling^{11,d}, I. B. Nikolaev^{10,b}, Z. Ning^{1,49}, S. Nisar^{8,l}, S. L. Olsen⁵⁴, Q. Ouyang^{1,49,54}, S. Pacetti^{23B,23C}, X. Pan^{9,f}, Y. Pan⁵⁸, A. Pathak¹, A. Pathak²⁷, P. Patteri^{23A}, M. Pelizaeus⁴, H. P. Peng^{63,49}, K. Peters^{11,d}, J. Pettersson⁶⁷, J. L. Ping³⁴, R. G. Ping^{1,54}, S. Pogodin²⁹, R. Poling⁵⁹, V. Prasad^{63,49}, H. Qi^{63,49}, H. R. Qi⁵², K. H. Qi²⁵, M. Qi³⁵, T. Y. Qi^{9,f}, S. Qian^{1,49}, W. B. Qian⁵⁴, Z. Qian⁵⁰, C. F. Qiao⁵⁴, L. Q. Qin¹², X. P. Qin^{9,f}, X. S. Qin⁴¹, Z. H. Qin^{1,49}, J. F. Qiu¹, S. Q. Qu⁵², S. Q. Qu³⁶, K. H. Rashid⁶⁵, K. Ravindran²¹, C. F. Redmer²⁸, A. Rivetti^{66C}, V. Rodin⁵⁵, M. Rolo^{66C}, G. Rong^{1,54}, Ch. Rosner¹⁵, M. Rump⁶⁰, H. S. Sang⁶³, A. Sarantsev^{29,c}, Y. Schelhaas²⁸, C. Schnier⁴, K. Schoenning⁶⁷, M. Scodreggio^{24A,24B}, D. C. Shan⁴⁶, W. Shan¹⁹, X. Y. Shan^{63,49}, J. F. Shangguan⁴⁶, M. Shao^{63,49}, C. P. Shen^{9,f}, H. F. Shen^{1,54}, P. X. Shen³⁶, X. Y. Shen^{1,54}, H. C. Shi^{63,49}, R. S. Shi^{1,54}, X. Shi^{1,49}, X. D. Shi^{63,49}, W. M. Song^{27,1}, Y. X. Song^{38,g}, S. Sosio^{66A,66C}, S. Spataro^{66A,66C}, K. X. Su⁶⁸, P. P. Su⁴⁶, G. X. Sun¹, H. K. Sun¹, J. F. Sun¹⁶, L. Sun⁶⁸, S. S. Sun^{1,54}, T. Sun^{1,54}, W. Y. Sun³⁴, W. Y. Sun²⁷, X. Sun^{20,h}, Y. J. Sun^{63,49}, Y. K. Sun^{63,49}, Y. Z. Sun¹, Z. T. Sun⁴¹, Y. H. Tan⁶⁸, Y. X. Tan^{63,49}, C. J. Tang⁴⁵, G. Y. Tang¹, J. Tang⁵⁰, J. X. Teng^{63,49}, V. Thoren⁶⁷, W. H. Tian⁴³, Y. Tian^{25,54}, I. Uman^{53B}, B. Wang¹, B. L. Wang⁵⁴, C. W. Wang³⁵, D. Y. Wang^{38,g}, H. J. Wang^{31,j,k}, H. P. Wang^{1,54}, K. Wang^{1,49}, L. L. Wang¹, M. Wang⁴¹, M. Z. Wang^{38,g}, Meng Wang^{1,54}, S. Wang^{9,f}, T. J. Wang³⁶, W. Wang⁵⁰, W. H. Wang⁶⁸, W. P. Wang^{63,49}, X. Wang^{38,g}, X. F. Wang^{31,j,k}, X. L. Wang^{9,f}, Y. Wang^{63,49}, Y. D. Wang³⁷, Y. F. Wang^{1,49,54}, Y. Q. Wang¹, Ying Wang⁵⁰, Z. Wang^{1,49}, Z. Y. Wang^{1,54}, Ziyi Wang⁵⁴, Zongyuan Wang^{1,54}, D. H. Wei¹², F. Weidner⁶⁰,

S. P. Wen¹, D. J. White⁵⁸, U. Wiedner⁴, G. Wilkinson⁶¹, M. Wolke⁶⁷, L. Wollenberg⁴, J. F. Wu^{1,54}, L. H. Wu¹, L. J. Wu^{1,54}, X. Wu^{9,f}, Z. Wu^{1,49}, L. Xia^{63,49}, T. Xiang^{38,g}, H. Xiao^{9,f}, S. Y. Xiao¹, Z. J. Xiao³⁴, X. H. Xie^{38,g}, Y. Xie⁴¹, Y. G. Xie^{1,49}, Y. H. Xie⁶, T. Y. Xing^{1,54}, C. J. Xu⁵⁰, G. F. Xu¹, Q. J. Xu¹⁴, W. Xu^{1,54}, X. P. Xu⁴⁶, Y. C. Xu⁵⁴, F. Yan^{9,f}, L. Yan^{9,f}, W. B. Yan^{63,49}, W. C. Yan⁷¹, Xu Yan⁴⁶, H. J. Yang^{42,e}, H. X. Yang¹, L. Yang⁴³, S. L. Yang⁵⁴, Yifan Yang^{1,54}, Zhi Yang²⁵, M. Ye^{1,49}, M. H. Ye⁷, J. H. Yin¹, Z. Y. You⁵⁰, B. X. Yu^{1,49,54}, C. X. Yu³⁶, G. Yu^{1,54}, J. S. Yu^{20,h}, T. Yu⁶⁴, C. Z. Yuan^{1,54}, L. Yuan², X. Q. Yuan^{38,g}, Y. Yuan^{1,54}, Z. Y. Yuan⁵⁰, C. X. Yue³², A. A. Zafar⁶⁵, X. Zeng Zeng⁶, Y. Zeng^{20,h}, A. Q. Zhang¹, B. X. Zhang¹, G. Y. Zhang¹⁶, H. Zhang⁶³, H. H. Zhang²⁷, H. H. Zhang⁵⁰, H. Y. Zhang^{1,49}, J. L. Zhang⁶⁹, J. Q. Zhang³⁴, J. W. Zhang^{1,49,54}, J. Y. Zhang¹, J. Z. Zhang^{1,54}, Jianyu Zhang^{1,54}, Jiawei Zhang^{1,54}, L. M. Zhang⁵², L. Q. Zhang⁵⁰, Lei Zhang³⁵, S. F. Zhang³⁵, Shulei Zhang^{20,h}, X. D. Zhang³⁷, X. Y. Zhang⁴¹, Y. Zhang⁶¹, Y. T. Zhang⁷¹, Y. H. Zhang^{1,49}, Yan Zhang^{63,49}, Yao Zhang¹, Z. Y. Zhang⁶⁸, G. Zhao¹, J. Zhao³², J. Y. Zhao^{1,54}, J. Z. Zhao^{1,49}, Lei Zhao^{63,49}, Ling Zhao¹, M. G. Zhao³⁶, Q. Zhao¹, S. J. Zhao⁷¹, Y. B. Zhao^{1,49}, Y. X. Zhao^{25,54}, Z. G. Zhao^{63,49}, A. Zhemchugov^{29,a}, B. Zheng⁶⁴, J. P. Zheng^{1,49}, Y. H. Zheng⁵⁴, B. Zhong³⁴, C. Zhong⁶⁴, H. Zhou⁴¹, L. P. Zhou^{1,54}, Q. Zhou^{1,54}, X. Zhou⁶⁸, X. K. Zhou⁵⁴, X. R. Zhou^{63,49}, X. Y. Zhou³², A. N. Zhu^{1,54}, J. Zhu³⁶, K. Zhu¹, K. J. Zhu^{1,49,54}, S. H. Zhu⁶², T. J. Zhu⁶⁹, W. J. Zhu³⁶, W. J. Zhu^{9,f}, Y. C. Zhu^{63,49}, Z. A. Zhu^{1,54}, B. S. Zou¹, J. H. Zou¹

(BESIII Collaboration)

¹ *Institute of High Energy Physics, Beijing 100049, People's Republic of China*

² *Beihang University, Beijing 100191, People's Republic of China*

³ *Beijing Institute of Petrochemical Technology, Beijing 102617, People's Republic of China*

⁴ *Bochum Ruhr-University, D-44780 Bochum, Germany*

⁵ *Carnegie Mellon University, Pittsburgh, Pennsylvania 15213, USA*

⁶ *Central China Normal University, Wuhan 430079, People's Republic of China*

⁷ *China Center of Advanced Science and Technology, Beijing 100190, People's Republic of China*

⁸ *COMSATS University Islamabad, Lahore Campus, Defence Road, Off Raiwind Road, 54000 Lahore, Pakistan*

⁹ *Fudan University, Shanghai 200433, People's Republic of China*

¹⁰ *G.I. Budker Institute of Nuclear Physics SB RAS (BINP), Novosibirsk 630090, Russia*

¹¹ *GSI Helmholtzcentre for Heavy Ion Research GmbH, D-64291 Darmstadt, Germany*

¹² *Guangxi Normal University, Guilin 541004, People's Republic of China*

¹³ *Guangxi University, Nanning 530004, People's Republic of China*

¹⁴ *Hangzhou Normal University, Hangzhou 310036, People's Republic of China*

¹⁵ *Helmholtz Institute Mainz, Staudinger Weg 18, D-55099 Mainz, Germany*

¹⁶ *Henan Normal University, Xinxiang 453007, People's Republic of China*

¹⁷ *Henan University of Science and Technology, Luoyang 471003, People's Republic of China*

¹⁸ *Huangshan College, Huangshan 245000, People's Republic of China*

¹⁹ *Hunan Normal University, Changsha 410081, People's Republic of China*

²⁰ *Hunan University, Changsha 410082, People's Republic of China*

²¹ *Indian Institute of Technology Madras, Chennai 600036, India*

²² *Indiana University, Bloomington, Indiana 47405, USA*

²³ *INFN Laboratori Nazionali di Frascati, (A)INFN Laboratori Nazionali di Frascati, I-00044, Frascati, Italy; (B)INFN Sezione di Perugia, I-06100, Perugia, Italy; (C)University of Perugia, I-06100, Perugia, Italy*

²⁴ *INFN Sezione di Ferrara, (A)INFN Sezione di Ferrara, I-44122, Ferrara, Italy; (B)University of Ferrara, I-44122, Ferrara, Italy*

²⁵ *Institute of Modern Physics, Lanzhou 730000, People's Republic of China*

²⁶ *Institute of Physics and Technology, Peace Ave. 54B, Ulaanbaatar 13330, Mongolia*

²⁷ *Jilin University, Changchun 130012, People's Republic of China*

²⁸ *Johannes Gutenberg University of Mainz, Johann-Joachim-Becher-Weg 45, D-55099 Mainz, Germany*

²⁹ *Joint Institute for Nuclear Research, 141980 Dubna, Moscow region, Russia*

³⁰ *Justus-Liebig-Universitaet Giessen, II. Physikalisches Institut, Heinrich-Buff-Ring 16, D-35392 Giessen, Germany*

³¹ *Lanzhou University, Lanzhou 730000, People's Republic of China*

³² *Liaoning Normal University, Dalian 116029, People's Republic of China*

³³ *Liaoning University, Shenyang 110036, People's Republic of China*

³⁴ *Nanjing Normal University, Nanjing 210023, People's Republic of China*

³⁵ *Nanjing University, Nanjing 210093, People's Republic of China*

- ³⁶ Nankai University, Tianjin 300071, People's Republic of China
- ³⁷ North China Electric Power University, Beijing 102206, People's Republic of China
- ³⁸ Peking University, Beijing 100871, People's Republic of China
- ³⁹ Qufu Normal University, Qufu 273165, People's Republic of China
- ⁴⁰ Shandong Normal University, Jinan 250014, People's Republic of China
- ⁴¹ Shandong University, Jinan 250100, People's Republic of China
- ⁴² Shanghai Jiao Tong University, Shanghai 200240, People's Republic of China
- ⁴³ Shanxi Normal University, Linfen 041004, People's Republic of China
- ⁴⁴ Shanxi University, Taiyuan 030006, People's Republic of China
- ⁴⁵ Sichuan University, Chengdu 610064, People's Republic of China
- ⁴⁶ Soochow University, Suzhou 215006, People's Republic of China
- ⁴⁷ South China Normal University, Guangzhou 510006, People's Republic of China
- ⁴⁸ Southeast University, Nanjing 211100, People's Republic of China
- ⁴⁹ State Key Laboratory of Particle Detection and Electronics, Beijing 100049, Hefei 230026, People's Republic of China
- ⁵⁰ Sun Yat-Sen University, Guangzhou 510275, People's Republic of China
- ⁵¹ Suranaree University of Technology, University Avenue 111, Nakhon Ratchasima 30000, Thailand
- ⁵² Tsinghua University, Beijing 100084, People's Republic of China
- ⁵³ Turkish Accelerator Center Particle Factory Group, (A)Istinye University, 34010, Istanbul, Turkey; (B)Near East University, Nicosia, North Cyprus, Mersin 10, Turkey
- ⁵⁴ University of Chinese Academy of Sciences, Beijing 100049, People's Republic of China
- ⁵⁵ University of Groningen, NL-9747 AA Groningen, The Netherlands
- ⁵⁶ University of Hawaii, Honolulu, Hawaii 96822, USA
- ⁵⁷ University of Jinan, Jinan 250022, People's Republic of China
- ⁵⁸ University of Manchester, Oxford Road, Manchester, M13 9PL, United Kingdom
- ⁵⁹ University of Minnesota, Minneapolis, Minnesota 55455, USA
- ⁶⁰ University of Muenster, Wilhelm-Klemm-Str. 9, 48149 Muenster, Germany
- ⁶¹ University of Oxford, Keble Rd, Oxford, UK OX13RH
- ⁶² University of Science and Technology Liaoning, Anshan 114051, People's Republic of China
- ⁶³ University of Science and Technology of China, Hefei 230026, People's Republic of China
- ⁶⁴ University of South China, Hengyang 421001, People's Republic of China
- ⁶⁵ University of the Punjab, Lahore-54590, Pakistan
- ⁶⁶ University of Turin and INFN, (A)University of Turin, I-10125, Turin, Italy; (B)University of Eastern Piedmont, I-15121, Alessandria, Italy; (C)INFN, I-10125, Turin, Italy
- ⁶⁷ Uppsala University, Box 516, SE-75120 Uppsala, Sweden
- ⁶⁸ Wuhan University, Wuhan 430072, People's Republic of China
- ⁶⁹ Xinyang Normal University, Xinyang 464000, People's Republic of China
- ⁷⁰ Zhejiang University, Hangzhou 310027, People's Republic of China
- ⁷¹ Zhengzhou University, Zhengzhou 450001, People's Republic of China
- ^a Also at the Moscow Institute of Physics and Technology, Moscow 141700, Russia
- ^b Also at the Novosibirsk State University, Novosibirsk, 630090, Russia
- ^c Also at the NRC "Kurchatov Institute", PNPI, 188300, Gatchina, Russia
- ^d Also at Goethe University Frankfurt, 60323 Frankfurt am Main, Germany
- ^e Also at Key Laboratory for Particle Physics, Astrophysics and Cosmology, Ministry of Education; Shanghai Key Laboratory for Particle Physics and Cosmology; Institute of Nuclear and Particle Physics, Shanghai 200240, People's Republic of China
- ^f Also at Key Laboratory of Nuclear Physics and Ion-beam Application (MOE) and Institute of Modern Physics, Fudan University, Shanghai 200443, People's Republic of China
- ^g Also at State Key Laboratory of Nuclear Physics and Technology, Peking University, Beijing 100871, People's Republic of China
- ^h Also at School of Physics and Electronics, Hunan University, Changsha 410082, China
- ⁱ Also at Guangdong Provincial Key Laboratory of Nuclear Science, Institute of Quantum Matter, South China Normal University, Guangzhou 510006, China

^j Also at Frontiers Science Center for Rare Isotopes, Lanzhou University, Lanzhou 730000, People's Republic of China

^k Also at Lanzhou Center for Theoretical Physics, Lanzhou University, Lanzhou 730000, People's Republic of China

^l Also at the Department of Mathematical Sciences, IBA, Karachi, Pakistan

Using an electron-positron collision data sample corresponding to an integrated luminosity of 2.93 fb^{-1} collected with the BESIII detector at a center-of-mass energy of 3.773 GeV , we search for the baryon-number and lepton-number violating decays $D^0 \rightarrow \bar{p}e^+$ and $D^0 \rightarrow pe^-$. No obvious signals are found with the current statistics. The upper limits on the branching fractions for $D^0 \rightarrow \bar{p}e^+$ and $D^0 \rightarrow pe^-$ are set to be 1.2×10^{-6} and 2.2×10^{-6} at 90% confidence level, respectively.

PACS numbers: 13.20.Fc, 12.15.Hh

I. INTRODUCTION

As demonstrated by the stability of ordinary matter, baryon number (B) is empirically known to be conserved to a very high degree. However, the absolute conservation of B has been questioned for many years. For example, the fact that there is an excess of baryons over antibaryons in the Universe implies the existence of baryon number violating (BNV) processes. Therefore, various extensions of the Standard Model (SM) with BNV processes have been proposed. At the level of dimension-six operators, BNV processes can happen with $\Delta(B - L) = 0$, where $\Delta(B - L)$ is the change of baryon number minus lepton number between initial and final states [1]. Another class of BNV operators are the dimension-seven operators allowing $\Delta(B - L) = 2$ processes [2]. Some of the SM extensions, *e.g.*, SU(5), SO(10), E6 and flipped SU(5) models, predict branching fractions (BFs) for these kinds of decays at the level of 10^{-39} to 10^{-27} [3, 4], compatible with the experimental limits from proton decay experiments.

For decades, the decay of the proton, the lightest baryon, has been searched for without success. An alternative probe is to look for the BNV decays of a heavy quark. In 2009, the CLEO collaboration searched for the decays of $D^0(\bar{D}^0) \rightarrow \bar{p}e^+$ and $D^0(\bar{D}^0) \rightarrow pe^-$ [5] and set upper limits (ULs) on the BFs to be $\mathcal{B}(D^0(\bar{D}^0) \rightarrow \bar{p}e^+) < 1.1 \times 10^{-5}$ and $\mathcal{B}(D^0(\bar{D}^0) \rightarrow pe^-) < 1.0 \times 10^{-5}$ at 90% confidence level (CL), respectively. For this result, the initial flavor (D^0 vs. \bar{D}^0) of the charm meson was not determined. The Feynman diagrams in Fig. 1 [5] show some of the possible mechanisms of $D^0 \rightarrow \bar{p}e^+$ based on analogous couplings of $p \rightarrow e^+\pi^0$ in SU(5) which is suggested by Biswal *et al* [5, 6]. However, there is no tree-level diagram for $D^0 \rightarrow pe^-$ in SU(5). These decays can be mediated by heavy hypothetical gauge bosons X and Y which have electric charge $\frac{4}{3}e$ or $\frac{1}{3}e$ and can couple a quark to a lepton. Hence, these bosons are sometimes called ‘‘leptoquarks’’. Various BNV processes were searched for in τ , Λ , D and B decays by the CLEO [7], CLAS [8] and BaBar [9] experiments, but no evidence was found. The large data samples accumulated by the BESIII experiment lead to the best sensitivity for investigating BNV decays of charmed mesons or charmonium states. The BESIII collaboration searched for BNV in $D^+ \rightarrow \bar{\Lambda}(\bar{\Sigma}^0)e^+$ [10] and $J/\psi \rightarrow \Lambda_c^+ e^- +$

c.c [11] and set ULs at the level of $10^{-8} - 10^{-6}$ with no significant signals.

In this paper, we present the most accurate search to date for the decays $D^0 \rightarrow pe^-$ and $D^0 \rightarrow \bar{p}e^+$ performed with an e^+e^- collision data sample corresponding to an integrated luminosity of 2.93 fb^{-1} [12] taken at a center-of-mass (CM) energy of 3.773 GeV with the BESIII detector. Throughout this paper, charge conjugate channels are always implied.

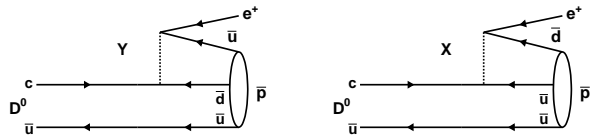


Fig. 1. Feynman diagrams of $D^0 \rightarrow \bar{p}e^+$ based on a leptoquark scenario.

II. BESIII DETECTOR AND MONTE CARLO SIMULATION

The BESIII detector is a magnetic spectrometer [13] located at the Beijing Electron Positron Collider (BEPCII) [14]. The cylindrical core of the BESIII detector consists of a helium-based multilayer drift chamber (MDC), a plastic scintillator time-of-flight system (TOF), and a CsI(Tl) electromagnetic calorimeter (EMC), which are all enclosed in a superconducting solenoidal magnet providing a 1.0 T magnetic field. The solenoid is supported by an octagonal flux-return yoke with resistive plate counter muon identifier modules interleaved with steel. The acceptance of charged particles and photons is 93% over 4π solid angle. The charged-particle momentum resolution at $1 \text{ GeV}/c$ is 0.5%, and the specific energy loss (dE/dx) resolution is 6% for the electrons from Bhabha scattering. The EMC measures photon energies with a resolution of 2.5% (5%) at 1 GeV in the barrel (end cap) region. The time resolution of the TOF barrel part is 68 ps, while that of the end cap part is 110 ps.

Monte Carlo (MC) simulated data samples produced with a GEANT4-based [16] package, which includes the

geometric description of the BESIII detector and the detector response, are used to determine the detection efficiency and to estimate the backgrounds. The simulation includes the beam energy spread and initial state radiation (ISR) in the e^+e^- annihilations modeled with the generator KKMC [17]. The inclusive MC samples consist of the production of $D\bar{D}$ pairs with consideration of quantum coherence for all neutral D modes, the non- $D\bar{D}$ decays of the $\psi(3770)$, the ISR production of the J/ψ and $\psi(3686)$ states, and the continuum processes. The known decay modes are modeled with EVTGEN [18] using the BFs taken from the Particle Data Group [19], and the remaining unknown decays from the charmonium states with LUNDCHARM [20]. The final state radiations from charged final state (FSR) particles are incorporated with the PHOTOS package [21].

III. DATA ANALYSIS

A. Method

At $\sqrt{s} = 3.773$ GeV, $D^0\bar{D}^0$ meson pairs are produced from $\psi(3770)$ decays without accompanying hadron(s). This offers an ideal platform to investigate the rare decays of D^0 in a very low background environment by using the double-tag (DT) method [22].

An event where a \bar{D}^0 is reconstructed via the hadronic decay modes of $\bar{D}^0 \rightarrow K^+\pi^-$, $K^+\pi^-\pi^0$ or $K^+\pi^-\pi^-\pi^+$ is called a single-tag (ST) candidate event. For fully-reconstructed STs, the remaining tracks and showers originate from the other meson, the D^0 . An event in which the decays of the D^0 and \bar{D}^0 are both reconstructed is called a DT candidate event. In this work, we search for the events with D^0 decays into $\bar{p}e^+$ or pe^- and \bar{D}^0 decays into one of the above three hadronic channels. The BFs for $D^0 \rightarrow \bar{p}e^+$ and $D^0 \rightarrow pe^-$ can be determined by

$$\mathcal{B}_{\text{sig}} = \frac{N_{\text{DT}}}{N_{\text{ST}} \cdot \epsilon_{\text{sig}}}, \quad (1)$$

where N_{ST} and N_{DT} are the yields of the ST \bar{D}^0 mesons and the DT events in data, respectively; ϵ_{sig} is the probability to reconstruct the signal under the condition that ST side was already reconstructed.

B. ST selection

The ST \bar{D}^0 candidates are selected with the same criteria as used in our previous works [25–34]. For each charged track, the polar angle with respect to the MDC axis (θ) is required to satisfy $|\cos\theta| < 0.93$, and the point of closest approach to the interaction point must be within 1 cm in the plane perpendicular to the MDC axis and within ± 10 cm along the MDC axis. Charged tracks are identified by using combined likelihoods from

the dE/dx and TOF measurements. Tracks are assigned as a pion (kaon) when that likelihood is larger than that for the kaon (pion) hypotheses.

Neutral pion candidates are reconstructed via $\pi^0 \rightarrow \gamma\gamma$ decay, where the photon candidates are chosen from the EMC showers. The EMC time deviation from the event start time is required to be within $[0, 700]$ ns. The energy deposited in the EMC is required to be greater than 25 (50) MeV if the crystal with the maximum deposited energy in that cluster is in the barrel (end cap) region [35]. The opening angle between the photon candidate and the nearest charged track is required to be greater than 10° . For any π^0 candidate, the invariant mass of the photon pair is required to be within $(0.115, 0.150)$ GeV/ c^2 . To improve the momentum resolution, a mass-constrained fit to the nominal π^0 mass [19] is imposed on the photon pair. The four-momentum of the π^0 candidate returned by this fit is used for further analysis.

In the selection of $\bar{D}^0 \rightarrow K^+\pi^-$ events, the backgrounds from cosmic rays and Bhabha events are rejected by using the same requirements described in Ref. [36]. To separate the ST \bar{D}^0 mesons from combinatorial backgrounds, we define the energy difference $\Delta E \equiv E_{\bar{D}^0} - E_{\text{beam}}$ and the beam-constrained mass $M_{\text{BC}} \equiv \sqrt{E_{\text{beam}}^2/c^4 - |\vec{p}_{\bar{D}^0}|^2/c^2}$, where E_{beam} is the beam energy, and $E_{\bar{D}^0}$ and $\vec{p}_{\bar{D}^0}$ are the total energy and momentum of the ST \bar{D}^0 meson candidate in the e^+e^- CM frame. If there is more than one \bar{D}^0 candidate combination in a specific tag mode, the one with the smallest $|\Delta E|$ is kept for further analysis.

To suppress combinatorial backgrounds in the M_{BC} distributions, the ST \bar{D}^0 candidates are required to fall in $\Delta E \in (-55, 40)$ MeV and $\Delta E \in (-25, 25)$ MeV for the tag modes with and without a π^0 in the final states, respectively. The M_{BC} distributions for various tag modes are shown in Fig. 2. For each tag mode, the yield of the ST \bar{D}^0 mesons is obtained by a fit to the corresponding M_{BC} distribution. The signal is described by a probability density function (PDF) determined from the MC simulation (MC-determined PDF) convolved with a double-Gaussian function which describes the resolution difference between data and MC simulation. The background is parametrized by an ARGUS function [37]. All parameters are left free in the fits. Figure 2 shows the fit results to the M_{BC} distributions for individual ST modes. The candidates located in the M_{BC} signal region of $(1.859, 1.873)$ GeV/ c^2 are kept for further analysis. Summing over the three tag modes gives the total yield of the ST \bar{D}^0 mesons to be 2321009 ± 1875 , where the uncertainty is calculated by the weighted average according to the fit results of the three tag modes.

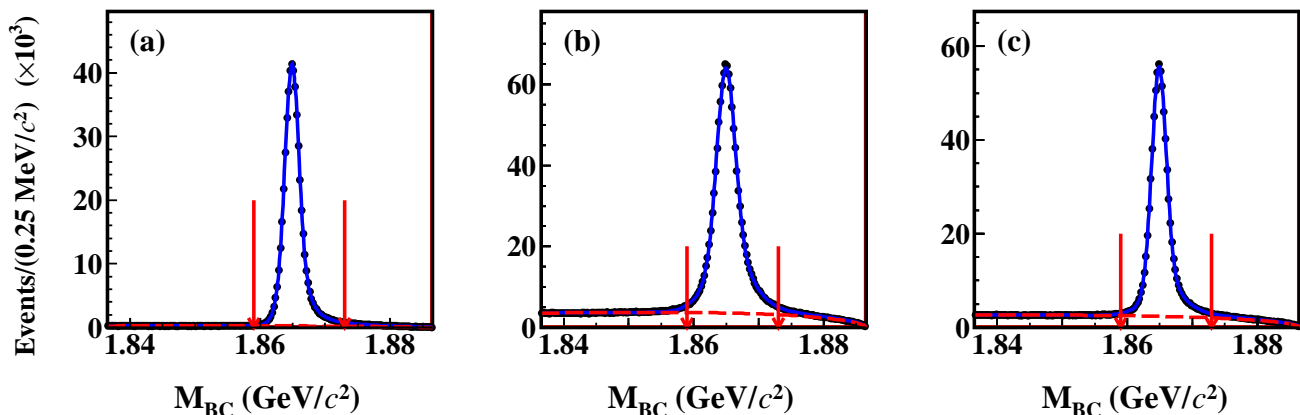


Fig. 2. Fits to the M_{BC} distributions of the ST \bar{D}^0 candidates for (a) $\bar{D}^0 \rightarrow K^+\pi^-$, (b) $\bar{D}^0 \rightarrow K^+\pi^-\pi^0$, and (c) $\bar{D}^0 \rightarrow K^+\pi^+\pi^-\pi^-$, respectively. In each plot, the points with error bars are data, the red dashed curve is the background contribution, and the blue solid line shows the total fit. Pairs of red arrows show the M_{BC} signal windows.

C. DT selection

To avoid possible bias, a blind analysis technique is followed where the data are analyzed only after the analysis procedure is fixed and validated with MC simulation. The candidates for $D^0 \rightarrow \bar{p}e^+$ and $D^0 \rightarrow pe^-$ are selected from the remaining tracks and showers in the presence of the tagged D^0 candidates. To obtain the information of $D^0 \rightarrow \bar{p}e^+$ and $D^0 \rightarrow pe^-$, we define ΔE^{sig} and M_{BC}^{sig} of the signal side similarly to those in the tag side.

Particle identification (PID) for electrons and positrons is performed by combining the dE/dx , TOF, and EMC measurements into confidence levels (CL) CL_K , CL_π , CL_p and CL_e for the kaon, pion, proton, and electron hypotheses. Electron (positron) candidates are required to satisfy $CL_e > 0.001$ and

$$\frac{CL_e}{CL_e + CL_\pi + CL_K} > 0.8. \quad (2)$$

To further suppress backgrounds due to misidentification between electrons (positrons) and hadrons, the ratio of the energy deposited in the EMC by the electron (positron) over its momentum (E/p) is required to be larger than $0.85c$. To partially recover the effects of FSR and bremsstrahlung (FSR recovery), the four-momenta of clusters in the EMC within 10° of the initial positron direction are added to the positron four-momentum measured by the MDC.

The proton or anti-proton candidates are identified by using the dE/dx and TOF measurements, from which combined confidence levels CL_K , CL_π , and CL_p for the kaon, pion, and proton hypotheses are calculated, respectively. The (anti-)proton candidates are required to satisfy $CL_p > 0.001$, $CL_p > CL_K$, and $CL_p > CL_\pi$.

Studies of MC samples show that there remain a few backgrounds coming from mis-reconstructed proton

candidates, *e.g.*, $D^0 \rightarrow K^-e^+\nu_e$ and processes other than $\psi(3770) \rightarrow D\bar{D}$. To suppress the background from $D^0 \rightarrow K^-e^+\nu_e$, we define a variable of $U_{\text{miss}} \equiv E_{\text{miss}} - |\vec{p}_{\text{miss}}| \cdot c$, where E_{miss} and \vec{p}_{miss} are the missing energy and momentum of the DT event in the e^+e^- CM frame, respectively. They are calculated by $E_{\text{miss}} \equiv E_{\text{beam}} - E_{K^-} - E_{e^+}$ and $\vec{p}_{\text{miss}} \equiv \vec{p}_{D^0} - \vec{p}_{K^-} - \vec{p}_{e^+}$, where $E_{K^-(e^+)}$ and $\vec{p}_{K^-(e^+)}$ are the measured energy and momentum of the K^- (e^+) candidates, respectively, and $\vec{p}_{D^0} \equiv -\hat{p}_{D^0} \cdot \sqrt{E_{\text{beam}}^2/c^2 - m_{D^0}^2} \cdot c^2$, where \hat{p}_{D^0} is the unit vector in the momentum direction of the ST \bar{D}^0 meson and m_{D^0} is the nominal \bar{D}^0 mass [19]. The use of the beam energy and the nominal D^0 mass for the magnitude of the ST D^0 meson momentum improves the U_{miss} resolution. For the correctly reconstructed events of $D^0 \rightarrow K^-e^+\nu_e$, the U_{miss} peaks around zero. The background from $D^0 \rightarrow K^-e^+\nu_e$ is suppressed by requiring U_{miss} to be outside the range of $(-0.15, 0.15)$ GeV.

D. Signal extraction

Figures 3(a) and 3(b) show the distributions of M_{BC}^{sig} vs. ΔE^{sig} of the candidate events for $D^0 \rightarrow \bar{p}e^+$ and $D^0 \rightarrow pe^-$ selected from the data sample, respectively. The signal yields are obtained by counting the events and conservatively assuming that the background events are evenly distributed. Since both of the M_{BC}^{sig} and ΔE^{sig} distributions from signal MC events have an asymmetric shape, to get a higher efficiency the signal regions are defined as $M_{BC}^{\text{sig}} (-2.5\sigma_{M_{BC}}, 4.0\sigma_{M_{BC}})$ vs. $\Delta E^{\text{sig}} (-2.5\sigma_{\Delta E}, 2.0\sigma_{\Delta E})$, where $\sigma_{M_{BC}}$ and $\sigma_{\Delta E}$ are the standard deviation of M_{BC}^{sig} and ΔE^{sig} which are obtained by fits to the signal MC. The signal region is determined to be $1.860 < M_{BC}^{\text{sig}} < 1.872$ GeV/ c^2 and $-0.028 < \Delta E^{\text{sig}} < 0.018$ GeV for $D^0 \rightarrow \bar{p}e^+$ (pe^-). We

obtain the signal yields of the candidates for $D^0 \rightarrow \bar{p}e^+$ and $D^0 \rightarrow pe^-$ (N^{sig}) to be 0 and 1, respectively.

The background yields in the signal region are estimated by the events in sideband region. In the whole region of $1.8365 < M_{\text{BC}}^{\text{sig}} < 1.8865$ GeV/ c^2 and $-0.1 < \Delta E^{\text{sig}} < 0.1$ GeV, we take the area outside of the signal region as our sideband region. There are 3 and 5 background events in the sideband region (N^{BKG}), for $D^0 \rightarrow \bar{p}e^+$ and $D^0 \rightarrow pe^-$, respectively. The ratios of the signal region area over the sideband region area (R_{area}) for $D^0 \rightarrow \bar{p}e^+$ and $D^0 \rightarrow pe^-$ are both 0.0587. Multiplying N^{BKG} by R_{area} gives the expected background events in the signal region (N^{bkg}) to be 0.2 and 0.3 for $D^0 \rightarrow \bar{p}e^+$ and $D^0 \rightarrow pe^-$, respectively.

E. DT efficiency

To determine the detection efficiency, we simulate 100,000 events of $\bar{D}^0 \rightarrow K^+\pi^-(\pi^0, \pi^+\pi^-)$ vs. $D^0 \rightarrow \bar{p}e^+$ process and $\bar{D}^0 \rightarrow K^+\pi^-(\pi^0, \pi^+\pi^-)$ vs. $D^0 \rightarrow pe^-$ process for each tag mode, respectively, where $\bar{D}^0 \rightarrow K^+\pi^-$ and the signal modes are modeled with a phase space generator, $\bar{D}^0 \rightarrow K^+\pi^-\pi^0$ is modeled with the Dalitz [23] generator and $\bar{D}^0 \rightarrow K^+\pi^-\pi^+\pi^-$ are modeled with the partial wave analysis [24] generator using measured distributions. The efficiencies of finding $D^0 \rightarrow \bar{p}e^+$ or $D^0 \rightarrow pe^-$ in the presence of the ST \bar{D}^0 meson (ϵ^{sig}) are $(64.7 \pm 0.2)\%$ and $(64.9 \pm 0.2)\%$, respectively.

IV. SYSTEMATIC UNCERTAINTY

With the DT method, almost all systematic uncertainties related to the ST selection are cancelled and do not affect the BF measurement. Table 1 summarizes the remaining systematic uncertainties in the measurements of the BFs for $D^0 \rightarrow \bar{p}e^+$ and $D^0 \rightarrow pe^-$. They are calculated relative to the measured BFs and are discussed below.

The systematic uncertainty of the total yield of the ST \bar{D}^0 mesons ($N_{\text{ST}}^{\text{tot}}$) is estimated to be 0.5% [25–27].

The systematic uncertainties of e^\pm tracking and PID efficiencies are studied with a control sample of $e^+e^- \rightarrow \gamma e^+e^-$. The difference of the e^\pm tracking efficiencies between data and MC simulation, 1.0%, is assigned as the systematic uncertainty of the e^\pm tracking efficiency. The systematic uncertainty from the e^\pm PID efficiency is assigned to be 1.1% per e^\pm . Here, the obtained efficiencies in the control sample have been re-weighted to those in the signal decays in two dimensional (momentum and $\cos\theta$) distributions.

The systematic uncertainties of proton tracking and PID efficiencies are studied using the control sample of $e^+e^- \rightarrow \pi^+\pi^-p\bar{p}$. The systematic uncertainties of the proton tracking and PID efficiencies are assigned to be 1.0% and 2.8%, respectively.

To study the systematic uncertainties due to the signal region in $M_{\text{BC}}^{\text{sig}}$ and ΔE^{sig} , we use the control sample of the DT candidate events for $D^0 \rightarrow K^-K^+$. The $M_{\text{BC}}^{\text{sig}}$ and ΔE^{sig} distributions of data are modeled with the MC-determined PDF convolved with a Gaussian resolution function. After smearing the corresponding Gaussian resolution function for our signal MC events, the changes of the DT efficiencies 0.1% and 0.3% are taken as the systematic uncertainties of the $M_{\text{BC}}^{\text{sig}}$ and ΔE^{sig} window.

The uncertainty arising from limited MC statistics, 0.3% for each signal decay mode, is considered as a source of systematic uncertainty. The systematic uncertainty due to the FSR recovery is assigned to be 0.3% by referring to that in large sample of $D^0 \rightarrow K^-e^+\nu_e$ [38].

We use the control sample of $D^0 \rightarrow K^-e^+\nu_e$ to study the systematic uncertainties from U_{miss} requirement. Since the efficiency differences caused by U_{miss} requirement between data and MC are very small, we ignore this term of systematic uncertainty.

Adding these systematic uncertainties in quadrature gives the total systematic uncertainties (Δ_{syst}) in the measurements of the BFs for $D^0 \rightarrow \bar{p}e^+$ or $D^0 \rightarrow pe^-$ to be 3.5%.

Table 1. Relative systematic uncertainties (in %) in the BF measurements.

Decay	$D^0 \rightarrow \bar{p}e^+$	$D^0 \rightarrow pe^-$
$N_{\text{ST}}^{\text{tot}}$	0.5	0.5
e^\pm tracking	1.0	1.0
e^\pm PID	1.1	1.1
$p(\bar{p})$ tracking	1.0	1.0
$p(\bar{p})$ PID	2.8	2.8
$M_{\text{BC}}^{\text{sig}}$ requirement	0.1	0.1
ΔE^{sig} requirement	0.3	0.3
MC statistics	0.3	0.3
FSR recovery	0.3	0.3
Total (Δ_{syst})	3.5	3.5

V. RESULTS

The ULs on the numbers of signal events at 90% CL are calculated by using a frequentist method [39] with unbanded profile likelihood treatment of systematic uncertainties, as implemented by the TROLKE package in the ROOT software [40], with the numbers of N^{sig} , N^{bkg} , ϵ^{sig} , and Δ_{syst} documented above. Here, the numbers of the signal and background events are assumed to follow a Poisson distribution, and the detection efficiency is assumed to follow a Gaussian distribution.

The ULs on the BFs are calculated to be

$$\mathcal{B}_{D^0 \rightarrow \bar{p}e^+} < 1.2 \times 10^{-6}$$

and

$$\mathcal{B}_{D^0 \rightarrow pe^-} < 2.2 \times 10^{-6},$$

respectively.

VI. SUMMARY

In summary, by analyzing an e^+e^- annihilation data sample corresponding to an integrated luminosity of 2.93 fb^{-1} collected with the BESIII detector, we have searched for the SM forbidden decays $D^0 \rightarrow \bar{p}e^+$ and $D^0 \rightarrow pe^-$. No obvious signals have been observed. The ULs on $\mathcal{B}(D^0 \rightarrow \bar{p}e^+)$ and $\mathcal{B}(D^0 \rightarrow pe^-)$ at 90% CL are set to be 1.2×10^{-6} and 2.2×10^{-6} , respectively. Our ULs are the most stringent ones to date for these processes, but are still far above the prediction of the higher generation model [3, 4].

VII. ACKNOWLEDGEMENT

The BESIII collaboration thanks the staff of BEPCII and the IHEP computing center for their strong support. This work is supported in part by National Key R&D Program of China under Grants No. 2020YFA0406400 and No. 2020YFA0406300; National Natural Science Foundation of China (NSFC) under Grants No.

12035009, No. 11875170, No. 11475090, No. 11625523, No. 11635010, No. 11735014, No. 11822506, No. 11835012, No. 11935015, No. 11935016, No. 11935018, No. 11961141012, No. 12022510, No. 12025502, No. 12035013, No. 12061131003, No. 12192260, No. 12192261, No. 12192262, No. 12192263, No. 12192264, and No. 12192265; the Chinese Academy of Sciences (CAS) Large-Scale Scientific Facility Program; Joint Large-Scale Scientific Facility Funds of the NSFC and CAS under Grants Nos. U1732263, U1832207; CAS Key Research Program of Frontier Sciences under Grant No. QYZDJ-SSW-SLH040; 100 Talents Program of CAS; INPAC and Shanghai Key Laboratory for Particle Physics and Cosmology; ERC under Grant No. 758462; European Union Horizon 2020 research and innovation programme under Grant No. Marie Skłodowska-Curie grant agreement No 894790; German Research Foundation DFG under Grants Nos. 443159800, Collaborative Research Center CRC 1044, FOR 2359, GRK 214; Istituto Nazionale di Fisica Nucleare, Italy; Ministry of Development of Turkey under Grant No. DPT2006K-120470; National Science and Technology fund; Olle Engkvist Foundation under Grant No. 200-0605; STFC (United Kingdom); The Knut and Alice Wallenberg Foundation (Sweden) under Grant No. 2016.0157; The Royal Society, UK under Grants Nos. DH140054, DH160214; The Swedish Research Council; U. S. Department of Energy under Grants Nos. DE-FG02-05ER41374, DE-SC-0012069.

-
- [1] S. Weinberg, *Phys. Rev. Lett.* **43**, 1566 (1979).
 - [2] F. Wilczek and A. Zee, *Phys. Rev. Lett.* **88**, 311 (1979).
 - [3] H. Georgi and S. L. Glashow, *Phys. Rev. Lett.* **32**, 438 (1974).
 - [4] W. S. Hou, M. Nagashima, and A. Soddu, *Phys. Rev. D* **72**, 095001 (2005).
 - [5] P. Rubin *et al.* (CLEO Collaboration), *Phys. Rev. D* **79**, 097101 (2009).
 - [6] K. Biswal, L. Maharana and S. P. Misra, *Phys. Rev. D* **25** 266 (1982).
 - [7] R. Godang *et al.* (CLEO Collaboration), *Phys. Rev. D* **59**, 091303(1999).
 - [8] M. E. McCracken *et al.*, *Phys. Rev. D* **92**, 072002 (2015).
 - [9] P. del Amo Sanchez *et al.* (BaBar Collaboration), *Phys.Rev.D* **83**, 091101(2011).
 - [10] M. Ablikim, *et al.* (BESIII Collaboration), *Phys. Rev. D* **101**, 031102 (2020).
 - [11] M. Ablikim, *et al.* (BESIII Collaboration), *Phys. Rev. D* **99**, 072006 (2019).
 - [12] M. Ablikim *et al.* (BESIII Collaboration), *Chin. Phys. C* **37**, 123001 (2013); *Phys. Lett. B* **753**, 629 (2016).
 - [13] M. Ablikim *et al.* (BESIII Collaboration), *Nucl. Instrum. Meth. A* **614**, 345 (2010).
 - [14] C. Yu *et al.*, in proceedings of the 7th International Particle Accelerator Conference, p. TUYA01 (2016).
 - [15] M. Ablikim *et al.* (BESIII Collaboration), *Chin. Phys. C* **44**, 040001 (2020).
 - [16] S. Agostinelli *et al.* (GEANT4 Collaboration), *Nucl. Instrum. Meth. A* **506**, 250 (2003).
 - [17] S. Jadach, B. F. L. Ward, and Z. Was, *Comp. Phys. Commu.* **130**, 260 (2000); *Phys. Rev. D* **63**, 113009 (2001).
 - [18] D. J. Lange, *Nucl. Instrum. Meth. A* **462**, 152 (2001); R. G. Ping, *Chin. Phys. C* **32**, 599 (2008).
 - [19] P. A. Zyla *et al.* (Particle Data Group), *Prog. Theor. Exp. Phys.* **2020**, 083C01 (2020).
 - [20] J. C. Chen, G. S. Huang, X. R. Qi, D. H. Zhang, and Y. S. Zhu, *Phys. Rev. D* **62**, 034003 (2000).
 - [21] E. Richter-Was, *Phys. Lett. B* **303**, 163 (1993).
 - [22] R. M. Baltrusaitis *et al.* (MARK-III Collaboration), *Phys. Rev. Lett.* **56**, 2140 (1986); J. Adler *et al.* (MARK-III Collaboration), *Phys. Rev. Lett.* **60**, 89 (1988).
 - [23] J. C. Anjos *et al.* (E691 Collaboration), *Phys. Rev. D* **48**, 56 (1993).
 - [24] M. Ablikim *et al.* (BESIII Collaboration), *Phys. Rev. D* **95**, 072010 (2017).
 - [25] M. Ablikim *et al.* (BESIII Collaboration), *Eur. Phys. J. C* **76**, 369 (2016).
 - [26] M. Ablikim *et al.* (BESIII Collaboration), *Chin. Phys. C* **40**, 113001 (2016).
 - [27] M. Ablikim *et al.* (BESIII Collaboration), *Phys. Rev. Lett.* **121**, 171803 (2018).
 - [28] M. Ablikim *et al.* (BESIII Collaboration), *Phys. Rev. D* **101**, 052009 (2020).

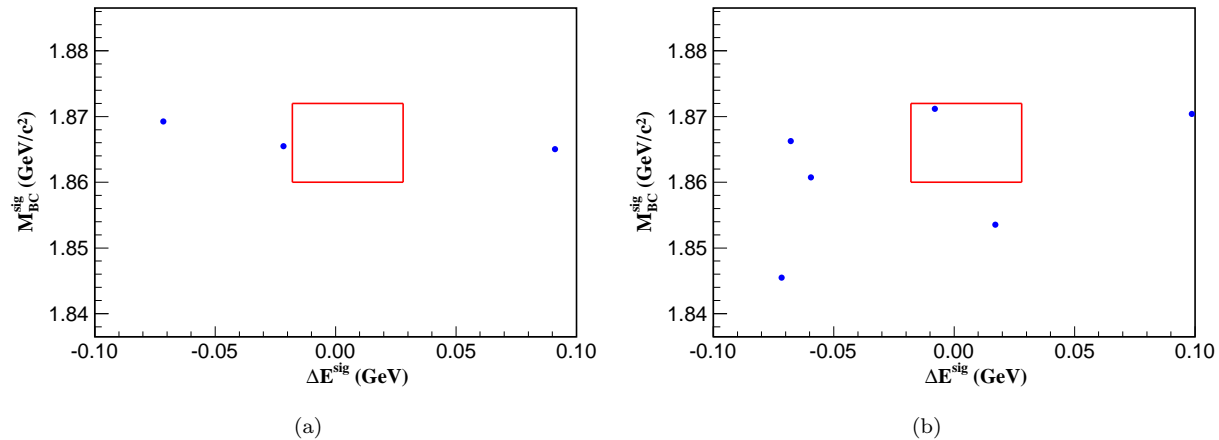


Fig. 3. Distributions of M_{BC}^{sig} vs. ΔE^{sig} of the candidate events for (a) $D^0 \rightarrow \bar{p}e^+$ and (b) $D^0 \rightarrow pe^-$ in data. The red rectangles denote the signal region.

- [29] M. Ablikim *et al.* (BESIII Collaboration), *Phys. Rev. D* **101**, 072005 (2020).
- [30] M. Ablikim *et al.* (BESIII Collaboration), *Phys. Rev. Lett* **124**, 231801 (2020).
- [31] M. Ablikim *et al.* (BESIII Collaboration), *Phys. Rev. Lett* **124**, 241803 (2020).
- [32] M. Ablikim *et al.* (BESIII Collaboration), *Phys. Rev. Lett.* **125**, 141802 (2020).
- [33] M. Ablikim *et al.* (BESIII Collaboration), *Phys. Rev. D* **102**, 052006 (2020).
- [34] M. Ablikim *et al.* (BESIII Collaboration), *Phys. Rev. D* **102**, 112005 (2020).
- [35] M. Ablikim *et al.* (BESIII Collaboration), *Nucl. Instr. Method A* **614**, 345 (2010).
- [36] M. Ablikim *et al.* (BESIII Collaboration), *Phys. Lett. B* **734**, 227 (2014).
- [37] H. Albrecht *et al.* (ARGUS Collaboration), *Phys. Lett. B* **241**, 278 (1990).
- [38] M. Ablikim *et al.* (BESIII Collaboration), *Phys. Rev. D.* **92**, 072012 (2015).
- [39] W. A. Rolke, A. M. Lopez, and J. Conrad, *Nucl. Instr. Methods Phys. Res., Sect. A* **551**, 493 (2005).
- [40] R. Brun and F. Rademakers, *Nucl. Instrum. Methods Phys. Res., Sect. A* **389**, 81 (1997).